


Article

Response of Nitrogen Metabolism in Masson Pine Needles to Elevated CO₂

Fan Wu ¹, Xiaobo Sun ¹, Xingfeng Hu ¹, Bingzhang Zou ², Nengqing Lin ², Jingquan Lin ² and Kongshu Ji ^{1,*}

¹ Key Laboratory of Forestry Genetics & Biotechnology of Ministry of Education, Co-Innovation Center for Sustainable Forestry in Southern China, Nanjing Forestry University, Nanjing 210037, China; eiknarf@126.com

² Baisha State-Owned Forest Farm, Shanghang 364200, China

* Correspondence: ksjj@njfu.edu.cn; Tel.: +86-025-85427308

Received: 6 February 2020; Accepted: 31 March 2020; Published: 1 April 2020



Abstract: To explore the response of nitrogen metabolism in Masson pine (*Pinus massoniana*) to high CO₂ concentrations, needles from one-year-old seedlings were used as materials to detect key enzyme activities, gene expression and different forms of nitrogen metabolites after CO₂ stress for different durations (0 h, 6 h, 12 h, 24 h). The results show that elevated CO₂ affected the efficiency of nitrogen metabolism in Masson pine needles, inhibiting the expression of key genes involved in nitrogen metabolism, including glutamate synthase (GOGAT), nitrite reductase (NiR), glutamine synthase (GS), nitrate reductase (NR) and glutamate dehydrogenase (GDH), and decreasing the activities of GOGAT, NiR, and GS. The decrease in enzyme activities and gene expression caused a decrease in different forms of nitrogen metabolites, including total nitrogen, ammonium, nitrite and specific amino acids. With prolonged stress, the nitrate content increased first and then decreased. In this study, the response pattern of nitrogen metabolism to CO₂ stress in Masson pine needles was described, which may aid future research on nitrogen utilization in Masson pine.

Keywords: masson pine; nitrogen metabolism; elevated CO₂; stress

1. Introduction

With the advent of the industrial revolution, the concentration of CO₂ in the atmosphere has increased as a result of human activities. According to the Global Carbon Project (GCP), the global atmospheric CO₂ concentration reached 407.38 ± 0.1 ppm averaged over 2018, and will rise to approximately 500 ppm by the middle of this century and to 700–1260 ppm by the end of this century [1,2]. The effect of increased CO₂ concentrations on the environment, especially on plants, is obvious because the rate at which plants adapt to CO₂ does not parallel the rate at which the CO₂ concentration increases [3,4].

In terms of plant nutrients, elevated CO₂ will accelerate the demands of plants for nutrients, and nitrogen is usually the limiting nutrient in plants [5,6]. The increase of CO₂ concentration in the environment enhanced the photosynthetic efficiency of plants, and the absorption and reduction of nitrogen elements in plants require energy and the reducing force provided by photosynthetic carbon metabolism, and the subsequent synthesis of various amino acids also requires a light reaction to provide a carbon skeleton [7,8]. Therefore, nitrogen metabolism in plants is closely related to photosynthetic carbon metabolism.

It is well known that the nitrogen absorbed by plants during the growth process mainly comes from two types of mineral nitrogen sources, ammonium (NH₄⁺) and nitrate (NO₃[−]). Studies have shown that different plants have different utilization efficiency of different forms of nitrogen under elevated

CO₂. For inorganic nitrogen, Men [9] found that the concentration of NO₃[−] and NH₄⁺ in leaves of winter wheat (*Triticum aestivum*) decreased under increased CO₂ conditions in an air chamber. Xu [10] also noted that an increase in the CO₂ concentration inhibited the reduction of NO₃[−] and reduced the nitrogen content in the flag leaves of winter wheat. For coniferous plants, Bassirrad et al. [11] and Su [12] showed that the NO₃[−] concentration in Loblolly pine (*Pinus taeda*) and Camphor pine (*Pinus sylvestris* var. *mongolica*) increased with the enrichment of atmospheric CO₂, while the NH₄⁺ concentration did not change significantly, and Johnson et al. [13] suggested that CO₂ stress would lead to a decrease in the concentration of NH₄⁺ in Ponderosa pine (*Pinus ponderosa*). According to previous reports, it can be seen that compared with crops, NO₃[−] may be a more nitrogen source that coniferous plants tend to use under CO₂ stress. In terms of amino acids, previous studies on species including rice (*Oryza sativa*) [14], European red pine (*Pinus sylvestris*) [15] and cotton (*Gossypium spp*) [16] indicated that elevated CO₂ would lead to the increase of amino acids. For the total nitrogen, Han [17], Wang [18] and Li [19] proved that enrichment CO₂ concentration would inhibit total nitrogen level in plants.

Regarding nitrogen assimilation, studies found that a high concentration of CO₂ could increase the activity of nitrate reductase (NR) or glutamine synthase (GS) in *Brassica napus* [20]. However, some scholars have noted that elevated CO₂ leads to decreased NR activity in wheat leaves [21]. Bauer [22] and Constable [23] confirmed that the increased CO₂ would not affect the NR activity of Eastern White Pine (*Pinus strobus*) and Loblolly pine. This may suggest that herbs have more plasticity in function than coniferous plants under increased CO₂ concentrations.

Masson pine (*Pinus massoniana*) is widely distributed in subtropical areas of China. Due to its tolerance to drought and barren lands, it has become the main pioneer tree species for afforestation and vegetation restoration in China [24,25]. At present, studies on nitrogen metabolism in Masson pine mainly focus on the effects of nitrogen deposition [26] and industrial pollution [27] on nitrogen distribution or the use of new technology to detect the nitrogen content in leaves [28]. However, few studies regarding nitrogen metabolism under CO₂ stress have been performed. Based on the previous research progress in conifers, we speculated that, when the environmental CO₂ concentration increased, the utilization efficiency of nitrogen in different forms would be different. Masson pine might be more inclined to use NO₃[−] as a nitrogen source. The content of amino acids would increase, and the total nitrogen level would decrease. In terms of enzyme activity, the activity of NR would not be affected by elevated CO₂, while that of other key enzymes would decrease or remained unchanged with the extension of treatment time. In addition, the response of key genes involved in the regulation of nitrogen metabolism to CO₂ stress has been rarely studied. Will their expression level be consistent with changes in enzyme activity and nitrogen content in different forms? In order to confirm the above hypothesis, in this study, Masson pine was exposed to high CO₂ concentrations, and the changes in nitrogen with different forms, in the corresponding regulatory enzymes activities and genes expression level were detected, to fill the gap in this field, reveal the influence of CO₂ stress on nitrogen transport and redistribution in Masson pine and to provide a scientific basis for fertilizer management and selection strategies in response to climate change.

2. Materials and Methods

2.1. Plant Materials and Experimental Design

One-year-old Masson pine seedlings, obtained from the seed orchard of the Baisha state-owned forest farm, Shanghang, Fujian Province, China (25°15′ N, 116°62′ E), were used in this study. Three individuals of the same clones with similar heights and uniform vigorous growth were chosen as the materials. After 10 days of recovery, the seedlings were subsequently moved into a growth chamber. The growth conditions were 10 h light/14 h dark cycles at 25 °C in the chamber. Air containing approximately 800–1000 ppm CO₂ (approximately two times the ambient CO₂ concentration) was aerated into the growth chamber constantly for at least 24 h. The CO₂ concentration in the chamber was monitored by an infrared CO₂ analysis reader (SenseAir, Delsbo, Sweden). Three biological replicates

for each treatment were sampled at 0 h (control check group, CK), 6 h, 12 h, 24 h, and every sample was divided into three parts, two of which were immediately stored in liquid nitrogen for RNA extraction and nitrogen metabolite analysis, and the other one was used for related enzyme activity detection.

2.2. Determination of the Content of Different Forms of Nitrogen

Samples with different treatment times were dried at 80 °C to a constant weight. Then, 0.2 g of sample was weighed, and the total nitrogen was determined by the Kjeldahl method [29].

Samples (1 g) treated with different stress treatment times were cut into pieces, ground with a small amount of double distilled water (ddH₂O) in a mortar, transferred into a dry triangular flask, supplemented with ddH₂O to a final volume of 20 mL, oscillated and finally allowed to rest for clarification. For NH₄⁺ determination, 5 mL of supernatant was extracted and placed in a 25 mL volumetric flask, and then 2.5 mL of reaction buffer A (0.1 M phenol, 0.3 mM sodium nitroprusside (Na₂Fe(CN)₅NO·2H₂O), stored in a brown bottle at 4 °C), 2.5 mL reaction buffer B (0.25 M NaOH, 0.05 M Na₂HPO₄, 0.2 M Na₃PO₄, 7 mM NaClO, stored in a brown bottle at 4 °C) and 0.5 mL masking agent (1.4 M Seignette salt (C₄H₁₂KNaO₁₀), 0.3 M EDTA-2Na, 0.05 M NaOH) were added. Then, the mixed solution was adjusted to 25 mL with ddH₂O and measured at 625 nm. For NO₃⁻ determination, 2 mL supernatant was extracted, and then, 18 mL acetic acid and 0.4 g mixed powder (BaSO₄: α-naphthylamine: zinc powder: p-aminobenzene sulfonic acid: MnSO₄: citric acid = 100:2:2:4:10:75) were added. Then, the mixture was vigorously shaken for 1 min and centrifuged at 4000 rpm for 5 min, and the supernatant was measured at 520 nm. For NO₂⁻, 5 mL supernatant was extracted and mixed with 0.2 mL chromogenic agent (0.58 M sulfanilamide (C₆H₈N₂O₂S), 15 mM hydrochloric acid *N*-(1-naphthyl) ethylenediamine (C₁₂H₁₄N₂·2HCl), 2 N H₃PO₄). Then, the mixed solution was adjusted to 25 mL with ddH₂O, allowed to stand for 1 h and measured at 543 nm [30].

2.3. Free Amino Acid Detection

A total of 20 mg of sample was weighed in a 2 mL microcentrifuge tube. After the addition of 400 µL of extraction buffer (acetonitrile: methanol: water, 2:2:1, containing adonitol 1 µg·mL⁻¹ as the internal standard), the samples were vortexed for 30 s, homogenized at 35 Hz for 4 min, and sonicated for 5 min in an ice-water bath. The homogenate and sonicate cycle was repeated 3 times, followed by incubation at -20 °C for 1 h and centrifugation at 12000 rpm and 4 °C for 15 min. The resulting supernatants were transferred to LC-MS vials and stored at -80 °C. The quality control sample was prepared by mixing an equal aliquot of the supernatants from all of the samples.

LC-MS/MS analyses were performed using a UHPLC system (1290, Agilent Technologies, Santa Clara, CA, USA) with a UPLC HSS T3 column (2.1 mm × 100 mm, 1.8 µm, Waters, Milford, MA, USA) coupled to Q Exactive (Orbitrap MS, Thermo, Waltham, MA, USA). Mobile phase A was 0.1% formic acid in water for the positive mode, and 5 mmol·L⁻¹ ammonium acetate in water for the negative mode. Mobile phase B was acetonitrile. The elution gradient was set as follows: 0 min, 1% B; 1 min, 1% B; 8 min, 99% B; 10 min, 99% B; 10.1 min, 1% B; and 12 min, 1% B. The flow rate was 0.5 mL·min⁻¹. The injection volume was 2 µL. The QE mass spectrometer was used for its ability to acquire MS/MS spectra on an information-dependent basis (IDA) during an LC/MS experiment. In this mode, the acquisition software Xcalibur version 4.0.27 (Thermo, Waltham, MA, USA) continuously evaluates the full-scan survey MS data as it collects and triggers the acquisition of MS/MS spectra depending on preselected criteria. Electron spray ionization (ESI) source conditions were set as follows: The sheath gas flow rate was 45 Arb, Aux gas flow rate was 15 Arb, capillary temperature was 400 °C, full MS resolution was 70,000, MS/MS resolution was 17,500, collision energy was 20/40/60 eV in the NCE model, and the spray voltage was 4.0 kV (positive) or -3.6 kV (negative).

2.4. Nitrogen Metabolism Enzyme Activities

The activity of glutamine synthase (GS) was determined by homogenizing the fresh sample (g) with the extraction buffer (0.05 M Tris-HCl, 2 mM Mg²⁺, 2 mM dithiothreitol (DTT), 0.4 M saccharose,

pH 8.0) at a 1:10 ratio in an ice-water bath and centrifuging for 10 min at 4000 rpm. Then, 400 μ L supernatant was mixed with 175 μ L reaction mixture (0.1 mM Tris-HCl, 80 mM Mg^{2+} , 20 mM sodium 2-aminopentanedioate ($C_5H_8NNaO_4$), 20 mM cysteine, 2 mM EDTA, 80 mM hydroxylamine hydrochloride (NH_3OHCl), pH 7.4), and reacted at 25 °C for 30 min. Then, 250 μ L chromogenic agent (0.2 M trichloroacetic acid (TCA), 0.37 M $FeCl_3$, 0.6 M HCl) was added. Samples were centrifuged at 4000 rpm for 5 min and the absorbance of γ -glutamylmonohydroxamate (γ -GHM) in the supernatant was measured at 540 nm. The activity determination of nitrate reductase (NR) was first mixed and homogenized 0.1 g fresh sample with 1 mL, 0.1 M phosphate buffer in ice-water bath, and the supernatant was obtained after centrifuging for 10 min at 4000 rpm. The reaction was incubated for 30 min at 25 °C after the addition of 100 μ L of enzyme extract to 500 μ L of reaction buffer (20 mM NADH, 20 mM KNO_3). The 500 μ L chromogenic agent (60 mM sulfanilic acid ($C_6H_7NO_3S$), 3 M HCl, 1.4 mM α -naphthylamine) was then added and the samples were measured colorimetrically at 540 nm after incubating for 20 min at 25 °C. The activities of glutamate dehydrogenase (GDH) and glutamate synthase (GOGAT) were determined by the decline rate of NADH absorbance at 340 nm in a reaction consisting of 900 μ L protein extract (0.1 g fresh sample added into 1 mL, 0.1 M Tris-HCl, pH 8.0, homogenizing in ice-water bath and then centrifuging for 10 min at 4000 rpm) and 100 μ L of reaction buffer for GDH (0.1 M Tris-HCl, 1.5 M NH_4Cl , 0.25 M α -ketoglutarate, 7.5 mM NADH, pH 8.0) or for GOGAT (0.1 M Tris-HCl, 10 mM dithiothreitol (DTT), 0.25 M α -ketoglutarate, 7.5 mM NADH, pH 8.6). For nitrite reductase (NiR) activity, the enzyme extract was obtained by homogenizing 0.1 g fresh sample and 1 mL extraction buffer (50 mM phosphate buffer, 1 mM EDTA, 3 mM cysteine, pH 7.5). Then, the reaction was incubated for 60 min at 25 °C after mixing 100 μ L enzyme extract with 400 μ L reaction buffer (50 mM Tris-HCl, 0.5 mM KNO_2 , 1 mM methylviologen, pH 7.5) and 120 μ L 0.12 M $Na_2S_2O_4$. The reaction was stopped by adding 200 μ L, 1 M zinc acetate. Then, 350 μ L supernatant was added with 700 μ L chromogenic agent (60 mM sulfanilic acid, 3 M HCl, 1.4 mM α -naphthylamine), and measured under 540 nm.

2.5. RNA Extraction, Complementary DNA (cDNA) Synthesis and Quantitative Real-Time PCR (qRT-PCR)

Total RNA from seedlings under four treatment conditions (0 h, 6 h, 12 h and 24 h) was extracted with three biological replicates for each treatment using the Plant RNA Isolation kit (Tiangen Biotech, Beijing, China). Then, first-strand cDNA was synthesized with FastKing gDNA Dispelling RT SuperMix (item number: KR118-02, Tiangen Biotech, Beijing, China) according to the manufacturer's instructions. For qRT-PCR, the mixtures consisted of 10 μ L of 2 \times ChamQTM Universal SYBR[®] qPCR Master Mix (item number: Q711-02, Vazyme Biotech, Nanjing, China), 0.4 μ L of forward primer and reverse primer, 2 μ L of cDNA, and 7.2 μ L of ddH₂O. The qRT-PCR program was set up in three stages: (1) 95 °C for 30 s (preincubation), (2) 95 °C for 10 s, 60 °C for 30 s, 72 °C for 30 s, repeated 40 times (amplification), (3) 95 °C for 15 s, 60 °C for 1 min and 95 °C for 15 s (melting curves). The qRT-PCR quality was estimated based on the melting curves. Alpha-tubulin (TUA) was used as the internal control [31]. The gene-specific primers employed are shown in Table 1. Three independent biological replicates and three technical replicates for each biological replicate were run. Quantification was achieved using comparative cycle threshold (Ct) values, and gene expression levels were calculated using the $2^{-\Delta\Delta Ct}$ method [31].

Table 1. Primers used in this study.

Primer		Sequence (5'→3')
qGS_F	Forward	GACTTCTGAACAGCAAAATGGTC
qGS_R	Reverse	GCAATCAGTTTAGATGGGCATAG
qNR_F	Forward	AACTGACAGCACTCTGAAACTCC
qNR_R	Reverse	AATATACATGTGGCCGTGAGAAG
qGDH_F	Forward	GGTCATTCTCCTGCAGTTGTTAC
qGDH_R	Reverse	ATGTTTCAGCTAACAAGGCTTCTG
qNiR_F	Forward	GAAGACGGGAGACATAGAGGACT
qNiR_R	Reverse	TAGATATAATCCGGGTCCACCTT
qGOGAT_F	Forward	CAAATTCAGTGTGTGCAGAGAG
qGOGAT_R	Reverse	AACAGCAACAGCAGCTACTTCTC

2.6. Statistical Analysis

The significance was determined by t-test using SPSS version 22.0 statistical software (IBM, New York, NY, USA) ($p < 0.05$). Differences in the effects of CO₂ on various treatments were determined by one-way ANOVA with Duncan's new multiple tests. The raw data of metabolite detection were converted into a common format, and adducts were achieved using XCMS online [32] (<http://metlin.scripps.edu/xcms/>), which provides a complete metabolomics workflow, including feature detection, retention time correction, alignment, annotation and analysis [32]. The ion strength of each detection peak was determined by combining the retention time and mass-to-charge ratio (m/z) values. The peak was detected, and the metabolite was obtained by the quartile interval denoising method; the missing value of the original data was obtained using half of the minimum value [33].

3. Results

3.1. Changes in Different N Forms under CO₂ Stress

As shown in Figure 1, different forms of nitrogen have different expression trends under CO₂ stress. Among them, there was no significant difference in the total nitrogen content in Masson pine needles after 6 h of treatment compared with 0 h of treatment. When treated for 12 h, the content decreased significantly and maintained a low level until 24 h (Figure 1A). The NO₃[−] content first increased with increasing treatment time, peaked at 6 h, and then continued to decline. The content was lower at 24 h than at 0 h (Figure 1B). The NO₂[−] content decreased rapidly in the early stage of treatment (6 h) and remained at a low level (Figure 1C), while NH₄⁺ showed a trend of continuous decrease (Figure 1D). In general, with increasing CO₂ stress treatments, different forms of nitrogen showed a downward trend.

3.2. Free Amino Acids

The changes in the contents of twenty common free amino acids under CO₂ stress are shown in Table 2. The contents of different amino acids in the elevated CO₂ environment were different. Among them, the contents of asparagine, histidine, arginine and tryptophan increased with increasing stress time and reached a maximum value at 24 h, while the content of amino acids such as glutamate, glutamine, proline and valine decreased with increasing treatment time; the difference between the different treatment times reached a significant level ($p < 0.05$). However, the change in concentration of aspartate, glycine, cysteine, phenylalanine, lysine and tyrosine showed no significant difference under CO₂ stress. The total amount of amino acids did not differ significantly at 0 h, 6 h and 12 h but increased significantly at 24 h (Table 2). In general, the amount of amino acids increased with increasing stress time.

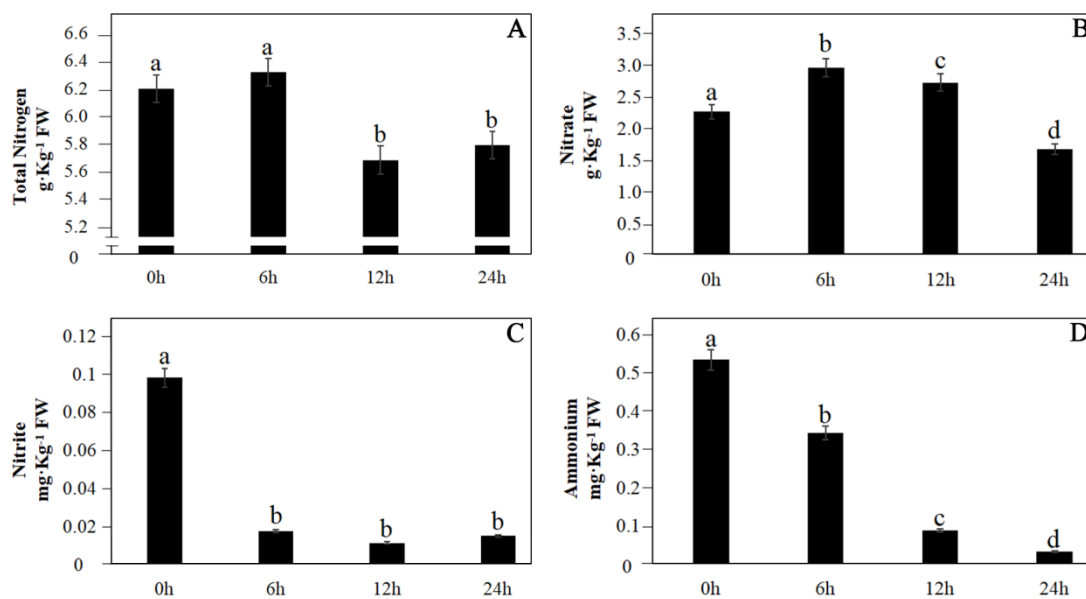


Figure 1. Effects of elevated CO₂ on different nitrogen forms. (A) Total nitrogen, (B) nitrate, (C) nitrite, (D) ammonium. Significant differences ($p < 0.05$) are indicated with lowercase letters. FW, fresh weight.

Table 2. Effect of elevated CO₂ on free amino acids.

	0 h	6 h	12 h	24 h
Aspartate	0.030 ± 0.002a	0.031 ± 0.052a	0.010 ± 0.052a	0.007 ± 0.001a
Serine	0.357 ± 0.124a	0.368 ± 0.156a	0.199 ± 0.074b	0.422 ± 0.084a
Threonine	0.366 ± 0.075b	0.490 ± 0.217b	0.563 ± 0.200b	1.111 ± 0.419a
Glutamate	4.086 ± 0.657a	3.387 ± 0.474ab	3.396 ± 0.860ab	2.555 ± 0.647b
Glycine	0.027 ± 0.006a	0.026 ± 0.005a	0.031 ± 0.010a	0.029 ± 0.005a
Alanine	0.116 ± 0.022b	0.267 ± 0.083a	0.232 ± 0.073a	0.275 ± 0.062a
Cysteine	0.010 ± 0.006a	0.008 ± 0.002a	0.010 ± 0.007a	0.011 ± 0.006a
Valine	0.592 ± 0.284a	0.34 ± 0.128b	0.215 ± 0.129b	0.243 ± 0.097b
Methionine	0.048 ± 0.021a	0.020 ± 0.007b	0.013 ± 0.001b	0.013 ± 0.004b
Isoleucine	0.002 ± 0.001a	0.001 ± 0.001b	0.002 ± 0.001ab	0.001 ± 0.001b
Phenylalanine	0.299 ± 0.061a	0.288 ± 0.055a	0.285 ± 0.167a	0.359 ± 0.162a
Lysine	0.500 ± 0.920a	0.556 ± 0.958a	0.492 ± 0.209a	0.517 ± 0.384a
Histidine	0.300 ± 0.084b	0.713 ± 0.528ab	0.622 ± 0.726ab	1.271 ± 0.994a
Arginine	1.748 ± 1.687b	4.616 ± 3.912ab	3.892 ± 5.721ab	7.702 ± 4.922a
Glutamine	5.793 ± 3.521a	3.734 ± 2.220ab	3.125 ± 1.090ab	1.895 ± 1.039b
Leucine	0.873 ± 0.186b	0.516 ± 0.144c	0.72 ± 0.173bc	1.327 ± 0.298a
Tyrosine	0.276 ± 0.071a	0.206 ± 0.096a	0.236 ± 0.090a	0.289 ± 0.113a
Tryptophan	1.414 ± 0.815b	1.794 ± 0.332ab	2.362 ± 0.909a	2.650 ± 0.537a
Proline	0.648 ± 0.202a	0.493 ± 0.151ab	0.483 ± 0.208ab	0.310 ± 0.071b
Asparagine	0.114 ± 0.056b	0.214 ± 0.091b	0.426 ± 0.336b	0.933 ± 0.733a
Total	17.572 ± 1.490b	18.068 ± 1.370b	17.314 ± 1.239b	21.230 ± 2.944a

Significant differences ($p < 0.05$) are indicated by lowercase letters.

3.3. Enzyme Activities and Gene Expression

An increase in the CO₂ concentration resulted in increased GDH (Figure 2A) and NR (Figure 2C) activities, among which GDH was significantly different between different treatments, while NR activity was only slightly upregulated after 6 h, and no significant difference existed between treatment groups. Other enzyme activities decreased with increasing stress time (Figure 2E,G,I), among which GS was the most obvious.

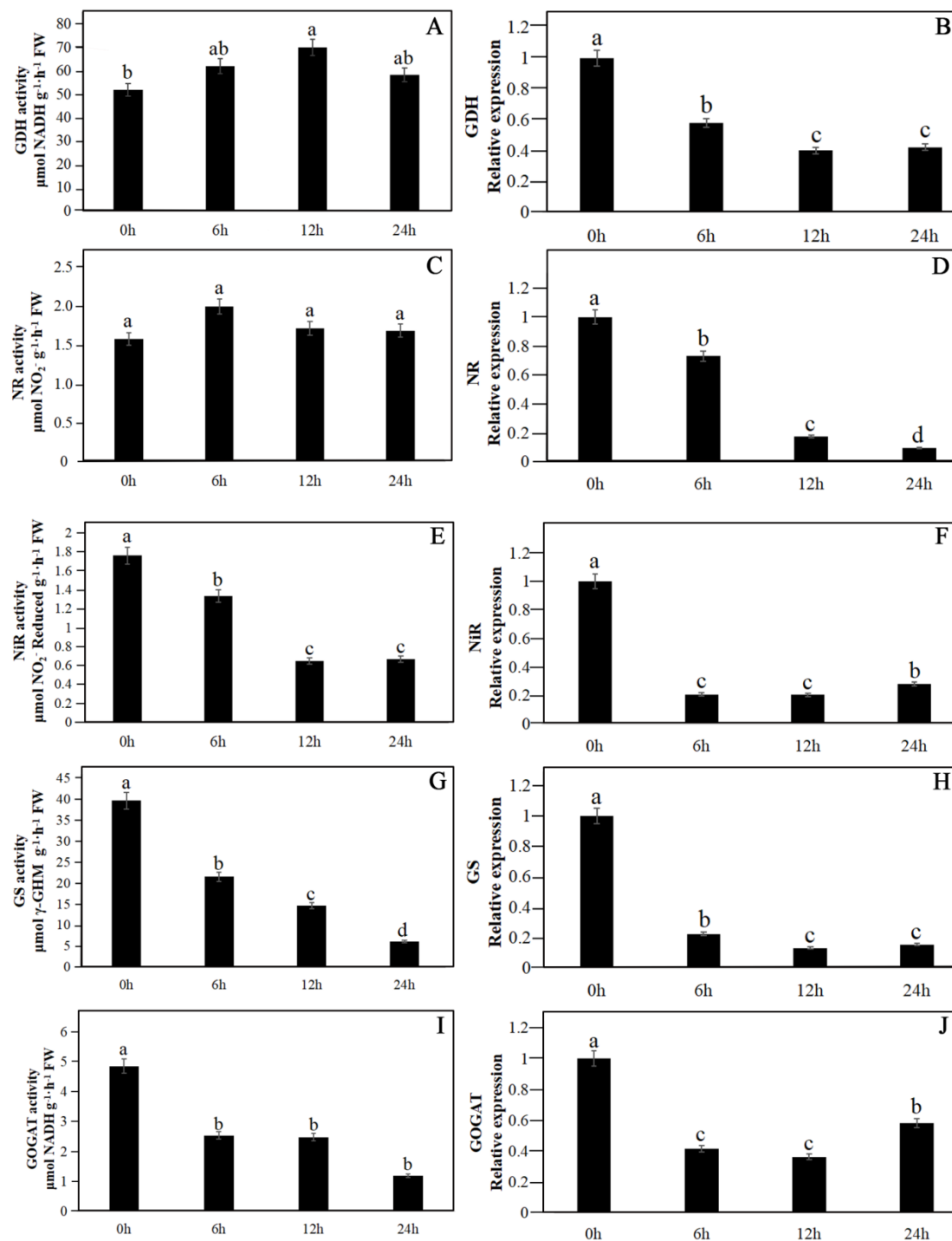


Figure 2. Response of nitrogen metabolic enzyme activities and gene expression changes in Masson pine needles at different times under CO₂ stress. Significant differences ($p < 0.05$) are indicated by lowercase letters. (A,B) Glutamate dehydrogenase (GDH), (C,D) nitrate reductase (NR), (E,F) nitrite reductase (NiR), (G,H) glutamine synthetase (GS), and (I,J) glutamate synthase (GOGAT). FW, fresh weight; γ -GHM, γ -glutamyl hydroxamate; NADH, nicotinamide adenine dinucleotide.

The expression patterns of key genes involved in nitrogen metabolism in a high CO₂ environment is shown in Figure 2. Among them, the expression of NR continued to decrease, reaching the lowest value at 24 h, and there was a significant difference between the expression levels corresponding to each treatment time node (Figure 2D). The expression trends of GDH and GS were similar. Their expression

levels no longer changed significantly after 12 h of stress treatment (Figure 2B,H). Interestingly, the expression levels of NiR and GOGAT decreased first, and there were no differences at 6 h and 12 h. However, after 24 h, the expression levels increased again but did not return to the untreated level (0 h). The expression levels at 24 h increased significantly compared with those at 6 h and 12 h (Figure 2F,J). Overall, the expression of all genes showed a downregulated trend with increased treatment time.

4. Discussion

4.1. Effects of Elevated CO₂ on Different Nitrogen Forms

Plants showed great flexibility and differences in the uptake and metabolism of different nitrogen forms under stress [34]. The results of this experiment show that with an increasing CO₂ concentration, the NO₃[−] content in Masson pine needles increased slightly in the early stage (0–12 h) and later (after 24 h) was lower than that in the control (0 h). Previous studies have found that when the concentration of CO₂ in the plasma membrane increases, the conversion efficiency of CO₂ to HCO₃[−] also increased at the same time, resulting in the difference between the concentration of HCO₃[−] inside and outside the plasma membrane. The absorption of NO₃[−] is coupled with the transmembrane exchange of HCO₃[−]. Therefore, with the outflow of HCO₃[−] in the plasma membrane, increasing NO₃[−] will enter the plasma membrane, leading to an increase in its content [35,36]. On the other hand, the contents of NO₂[−] and NH₄⁺ decreased continuously with increasing stress time, reaching the lowest value at 24 h (Figure 1C,D). Thornton [37] noted that plants had feedback regulation on the absorption and metabolism of NH₄⁺, NO₂[−] and NO₃[−]; therefore, an increase in the NO₃[−] content may cause a decrease in the other two forms of nitrogen. Furthermore, Ma [38] noted that an increase in the amino acid content would also inhibit the absorption and metabolism of inorganic nitrogen by plants. In general, the content of amino acids increased with increasing stress time and reached a maximum value at 24 h, particularly for threonine, arginine and tryptophan (Table 2). Therefore, the increase in the amino acid content may also be another explanation for the decline in the NH₄⁺, NO₂[−], and NO₃[−] contents after 24 h. In terms of the total nitrogen content, there was no significant change within 6 h; however, it began to decrease after 12 h and was lower at 12 h than at 0 h, eventually reaching a significant level. Studies have shown that an increase in the CO₂ concentration will reduce the total nitrogen concentration in plants [39,40], but the reasons vary in different reports. When Li [19] studied the change in the total nitrogen content in tea leaves under CO₂ and high temperature stress, he found that the decrease in the free amino acid and caffeine contents was the main reason for the decrease in the total nitrogen content. Weigel [41] believed that the decrease in total nitrogen was related to the increase in the carbohydrate content in plants. The results of our experiment show that the main reason for the decrease in the total nitrogen in Masson pine needles may be the decrease in the inorganic nitrogen content. Perhaps because of the different responses of different species to elevated CO₂ or the application of other stress treatments at the same time, there were differences in the reasons for the decrease in the total nitrogen content in leaves in different reports.

4.2. Enzyme Activities and Gene Expression Response to CO₂ Stress

According to the results of this experiment, NiR and GS activities decreased with increasing treatment time under CO₂ stress (Figure 2E,G). This would lead to a decrease in the contents of NH₄⁺ and glutamine, the products catalyzed by the two reactions. This inference was confirmed by the corresponding experimental results (Figure 1D, Table 2). When Li [42] studied the response of nitrogen metabolism in cucumber (*Cucumis sativus*) under CO₂ stress, the activity of NiR changed in a way that contrasts the changes in NiR activity in our study. It is possible that Li applied NaCl stress at the same time, resulting in inconsistent results. The response of GS was consistent with that reported in other species [43]. In addition, the activity of GOGAT showed a decreasing trend (Figure 2I), while GDH correspondingly increased at the same time (Figure 2A). GOGAT and GDH are two key enzymes involved in the transformation of α-ketoglutaric acid into glutamate in plant cells. GOGAT uses

glutamine as the nitrogen source for glutamate synthesis, while GDH uses NH_4^+ [44]. Our results showed that under CO_2 stress, the metabolic pathway of GOGAT was inhibited, and Masson pine synthesized glutamate mainly through the GDH pathway. Therefore, increasing NH_4^+ was consumed, leading to a decrease in its content (Figure 1D). On the other hand, there was no significant difference in the NR activity in each treatment, indicating that NR was not affected by CO_2 stress (Figure 2C). Interestingly, the NR response patterns were significantly different from those previously reported. The results of Torralbo et al. [45] were consistent with this experiment. Perez-Lopez et al. [46] noted that increasing the CO_2 concentration alone did not affect the activity of actual nitrate reductase (NRact). However, when NaCl stress was applied at the same time, the NRact activity increased. Zaghdoud et al. [47] showed the same NR activity response to CO_2 and drought stress as Usue. Anabel et al. [48] confirmed that NR activity showed a continuous increasing trend under drought and CO_2 stresses. These differences in results may be due to the differences in the materials and experimental designs used. Further experimental verification of the mechanism of NR activity under CO_2 stress is needed.

At the gene level, the results show that CO_2 enrichment comprehensively inhibited the expression of key genes involved in nitrogen metabolism (Figure 2B,D,F,H,G). This highlighted the phenomenon that CO_2 stress could damage nitrogen assimilation in Masson pine, which might be related to the carbon pool and source imbalance in needles [45]. Notably, when Vicente [49] studied the response mode of durum wheat nitrogen metabolism genes under the stress of nitrogen supply, temperature and CO_2 , he found that elevated CO_2 , atmospheric temperature and low N supply could induce the expression of GS and Fd-GOGAT with an upregulated trend, while the expression of other genes was inhibited. We speculated that the cross-talk mechanism between different stresses was the reason for this finding [50]. On the other hand, when we analyzed the correlation between genes and enzyme activities, we found that the enzyme activity and gene expression levels of NiR, GS and GOGAT showed a similar trend. They all decreased with the extension of treatment time. Interestingly, while the enzyme activity of NR remained unchanged, the gene expression decreased gradually (Figure 2C,D). In addition, GDH gene expression was gradually downregulated, while its enzyme activity increased (Figure 2A,B). The reason for the desynchronization of the NR gene and enzyme activity may be its complex stress mechanism. The reason for the difference between the gene expression and enzyme activity of GDH was speculated to be due to the presence of two types of GDH enzymes (NADH-GDH and NADPH-GDH) in plant cells [44], and the obtained enzyme activity data might contain both expression amounts, leading to an increase in the final amount.

Noteworthy, the previous studies have shown that the nitrogen fixation ability and the changes of nitrogen in plants are also affected by soil fertility [51,52], soil microorganisms [53,54] or metal elements [55]. We studied the change of elevated CO_2 content as the main factor but did not verify or discuss the influence of other factors on nitrogen metabolism of Masson pine under the same condition. With the increase of atmospheric CO_2 concentration, are there other factors that can affect nitrogen in Masson pine? What are their influence patterns and mechanisms? Is there any cross-talk between these factors? Perhaps all this needs to be proved by further research.

5. Conclusions

This study attempted to explore the response patterns of nitrogen metabolism in Masson pine needles to high CO_2 stress. The experimental results showed that elevated CO_2 led to an increase in the concentration of NO_3^- and amino acids and a decrease in the total nitrogen, inhibiting the key genes expression, decreasing the nitrogen metabolic enzymes activities except NR. The above results were consistent with the previous hypothesis. Noteworthy, GDH showed an increasing trend under the same conditions. We speculated that Masson pine mainly synthesized glutamic acid through the GDH pathway when CO_2 concentration increased (Figure 3). Additional studies on this phenomenon are needed. As the first report on the response of nitrogen metabolism to CO_2 stress in Masson pine needles, this study provides a valuable basis for further research in this area.

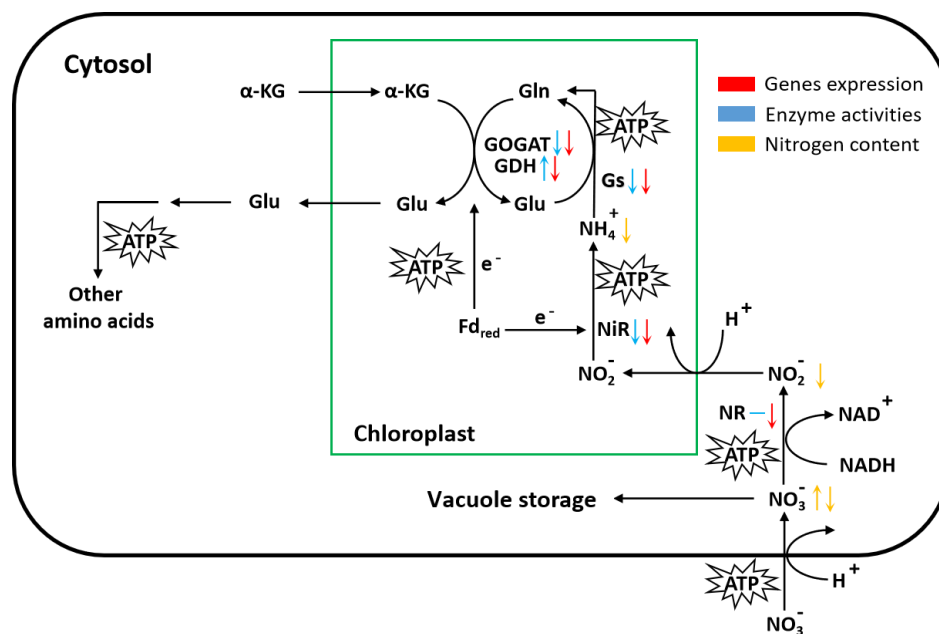


Figure 3. Influence of high CO₂ concentration on nitrogen metabolism regulation in Masson pine needles. Biosynthesis pathways according to Taiz [56]. The green and black rectangles represent the chloroplast and cytosol, respectively. The gene expression, enzyme activities and the content of different nitrogen forms are shown in red, blue and orange, respectively. Up- and downward-facing arrows indicate up- and downregulated expression, respectively. The blue line in NR indicates that there is no difference in the enzyme activity expression of NR, and the specific data are shown in Figure 1B. α-KG, α-Ketoglutaric acid; Fdred, Reduced ferredoxin.

Author Contributions: Conceptualization, F.W. and K.J.; software, X.H. and J.L.; investigation, W.F., N.L. and X.S.; resources, B.Z. and N.L.; writing—original draft preparation, F.W. and X.S.; writing—review and editing, F.W. and K.J.; visualization, F.W., J.L. All authors approved the final draft. All authors have read and agreed to the published version of the manuscript.

Funding: The research was financially supported by the National Key R&D Program of China (2017YFD0600304) and the Priority Academic Program Development of Jiangsu Higher Education Institutions (PAPD).

Conflicts of Interest: The authors declare that they have no competing interests.

References

- Gomez-Casanovas, N.; Blanc-Betes, E.; Gonzalez-Meler, M.; Azcon-Bieto, J. Changes in Respiratory Mitochondrial Machinery and Cytochrome and Alternative Pathway Activities in Response to Energy Demand Underlie the Acclimation of Respiration to Elevated CO₂ in the Invasive *Opuntia ficus-indica* [OA]. *Plant Physiol.* **2007**, *145*, 49–61. [CrossRef] [PubMed]
- GCP. Carbon Budget. Available online: <http://www.globalcarbonproject.org/carbonbudget> (accessed on 13 March 2020).
- Ehleringer, J.R.; Schulze, E.D. *Ecosystem Physiology Responses to Global Change*; Cambridge University Press: Cambridge, UK; London, UK, 1999; pp. 14–16.
- Wang, W.M.; Wang, C.; Li, C.J.; Lin, W.H. Effects of elevated atmospheric CO₂ concentrations on growth of plants. *Acta Bot. Boreal. Occident. Sin.* **2000**, *20*, 676–683.
- Thilakarathne, C.L.; Tausz-Posch, S.; Cane, K.; Norton, R.M.; Tausz, M.; Seneweera, S. Intraspecific variation in growth and yield response to elevated CO₂ in wheat depends on the differences of leaf mass per unit area. *Funct. Plant Biol.* **2013**, *40*, 185–194. [CrossRef]
- Wu, Q.; Zhang, C.; Yu, Z.; Zhang, J.; Zhu, C.; Zhao, Z.; Xiong, J.; Chen, J. Effects of elevated CO₂ and nitrogen addition on organic carbon and aggregates in soil planted with different rice cultivars. *Plant Soil* **2018**, *432*, 245–258. [CrossRef]

7. Kleinhofs, A.; Warner, R.L. *Advances in Nitrate Assimilation*; Elsevier BV: Amsterdam, The Netherlands, 1990; pp. 89–120.
8. Lea, P.J.; Robinson, S.A.; Stewart, G.R. *The Enzymology and Metabolism of Glutamine, Glutamate and Asparagine Intermediary Nitrogen Metabolism the Biochemistry of Plants*; Academic Press: New York, NY, USA, 2012; pp. 44–51.
9. Men, Z.H.; Li, S.X. Effect of CO₂ concentration on nitrogen metabolism of winter wheat. *Zhongguo Nongye Kexue* **2005**, *38*, 320–326.
10. Xu, Y.B. Effect of CO₂ Enrichment on Plant Growth and Nitrogen Use of Winter Wheat. Master's Thesis, Northwest Agriculture and Forestry University, Xianyang, China, 2012.
11. Bassirirad, H.; Thomas, R.B.; Reynolds, J.F. Differential responses of root uptake kinetics of NH₄⁺ and NO₃[−] to enriched atmospheric CO₂ concentration in field-grown loblolly pine. *Plant Cell Environ.* **1996**, *16*, 957–962. [[CrossRef](#)]
12. Su, W.L. Effects of Elevation CO₂ on Nitrogen Uptake Characteristic and Growth of *Larix Gmelinii* and *Pinus Sylvestris* var. Mongolica. Master's Thesis, Northeast Forestry University, Harbin, China, 2008.
13. Johnson, D.; Cheng, W.; Ball, J. Effects of CO₂ and N fertilization on decomposition and N immobilization in ponderosa pine litter. *Plant Soil* **2000**, *224*, 115–122. [[CrossRef](#)]
14. Pang, J.; Zhu, J.G.; Liu, G. Effects of free-air CO₂ enrichment (FACE) on concentrations of various N forms in rice tissues. *J. Agro-Environ. Sci.* **2005**, *24*, 833–837.
15. Johansson, E.M.; Fransson, P.M.A.; Finlay, R.D.; Van Hees, P. Quantitative analysis of soluble exudates produced by ectomycorrhizal roots as a response to ambient and elevated CO₂. *Soil Biol. Biochem.* **2009**, *41*, 1111–1116. [[CrossRef](#)]
16. Chen, F.J.; Ge, F.; Liu, X.H. Responses of cotton to elevated CO₂ and the effects on cotton aphid occurrences. *Acta Ecol. Sin.* **2004**, *24*, 991–996.
17. Han, X. Effects of Free Air CO₂ Enrichment on Wheat Growth and Yield: The Physiological Basis. Ph.D. Thesis, Chinese Academy of Agricultural Sciences, Beijing, China, 2012.
18. Wang, X.J. *Effect of CO₂ Enrichment on Growth, Root Uptake Characteristics and Efficiency in Oilseed Rape*; Hunan Agricultural University: Changsha, China, 2012.
19. Li, Z.X. Effects of Elevated CO₂ and Heat Stress on Growth and Development of Tea Plant. Master's Thesis, Chinese Academy of Agricultural Sciences, Beijing, China, 2016.
20. Yang, C.; Tan, T.; Zhang, L.; Yu, J.L.; Liao, Q.; Zhang, Z.H.; Liu, Q.; Rong, X.M.; Song, H.X.; Guan, C.Y. Effects of high CO₂ concentration in atmosphere on nitrogen assimilation and plant growth of Oilseeds Rape (*Brassica napus* L.). *Ecol. Environ. Sci.* **2013**, *22*, 1688–1694.
21. Hocking, P.; Meyer, C. Effects of CO₂ Enrichment and Nitrogen Stress on Growth, and Partitioning of Dry Matter and Nitrogen in Wheat and Maize. *Funct. Plant Biol.* **1991**, *18*, 339–356. [[CrossRef](#)]
22. Bauer, G.; Berntson, G.M. Ammonium and nitrate acquisition by plants in response to elevated CO₂ concentration: The roles of root physiology and architecture. *Tree Physiol.* **2001**, *21*, 137–144. [[CrossRef](#)] [[PubMed](#)]
23. Constable, J.V.H.; BassiriRad, H.; Lussenhop, J.; Zerihun, A. Influence of elevated CO₂ and mycorrhizae on nitrogen acquisition: Contrasting responses in *Pinus taeda* and *Liquidambar styraciflua*. *Tree Physiol.* **2001**, *21*, 83–91. [[CrossRef](#)] [[PubMed](#)]
24. Ni, Z.; Ye, Y.; Bai, T.; Xu, M.; Xu, L.-A. Complete Chloroplast Genome of *Pinus massoniana* (Pinaceae): Gene Rearrangements, Loss of *ndh* Genes, and Short Inverted Repeats Contraction, Expansion. *Molecules* **2017**, *22*, 1528. [[CrossRef](#)]
25. Ni, Z.; Zhou, P.; Xu, M.; Xu, L.-A. Development and characterization of chloroplast microsatellite markers for *Pinus massoniana* and their application in *Pinus* (Pinaceae) species. *J. Genet.* **2018**, *97*, 53–59. [[CrossRef](#)]
26. Zhang, Y.; Zhou, Z.; Yang, Q. Nitrogen (N) Deposition Impacts Seedling Growth of *Pinus massoniana* via N:P Ratio Effects and the Modulation of Adaptive Responses to Low P (Phosphorus). *PLoS ONE* **2013**, *8*, e79229. [[CrossRef](#)]
27. Guan, L.L.; Wen, D. More nitrogen partition in structural proteins and decreased photosynthetic nitrogen-use efficiency of *Pinus massoniana* under in situ polluted stress. *J. Plant Res.* **2011**, *124*, 663–673. [[CrossRef](#)]
28. Ni, C.; Wang, D.; Tao, Y. Variable weighted convolutional neural network for the nitrogen content quantization of Masson pine seedling leaves with near-infrared spectroscopy. *Spectrochim. Acta Part A: Mol. Biomol. Spectrosc.* **2019**, *209*, 32–39. [[CrossRef](#)]

29. Treder, K.; Wanic, M.; Jastrzebska, M. The Influence of interaction between spring wheat and spring barley on accumulation of nitrogen, phosphorus and potassium in plants. *Ann. UMCS, Agric.* **2009**, *64*, 94–106. [\[CrossRef\]](#)
30. Zhang, Z.L.; Li, X.F. *Experimental Guidance of Plant Physiology*; Higher Education Press: Beijing, China, 2016; pp. 36–48.
31. Zhu, P.; Ma, Y.; Zhu, L.; Chen, Y.; Li, R.; Ji, K.S.; Ji, K.S. Selection of Suitable Reference Genes in *Pinus massoniana* Lamb. Under Different Abiotic Stresses for qPCR Normalization. *Forests* **2019**, *10*, 632. [\[CrossRef\]](#)
32. XCMS. Meta XCMS. Available online: <http://metlin.scripps.edu/xcms> (accessed on 5 January 2020).
33. Li, M.; Li, Y.; Zhang, W.; Li, S.; Gao, Y.; Ai, X.; Zhang, D.; Liu, B.; Li, Q. Metabolomics analysis reveals that elevated atmospheric CO₂ alleviates drought stress in cucumber seedling leaves. *Anal. Biochem.* **2018**, *559*, 71–85. [\[CrossRef\]](#) [\[PubMed\]](#)
34. Andersen, K.; Mayor, J.R.; Turner, B.L. Plasticity in nitrogen uptake among plant species with contrasting nutrient acquisition strategies in a tropical forest. *Ecology* **2017**, *98*, 1388–1398. [\[CrossRef\]](#) [\[PubMed\]](#)
35. Marschner, H. Functions of mineral nutrients: Macronutrients. In *The Mineral Nutrition of Higher Plants*, 2nd ed.; Marschner, P., Ed.; Academic Press: New York, NY, USA, 1995; pp. 229–255.
36. Zhao, X. Effect of Elevated Root-Zone CO₂ Concentration on Melon Seeding Nitrogen Absorption, Metabolism and Transport in Root. Master's Thesis, Shenyang Agricultural University, Shenyang, China, 2012.
37. Thornton, B.; Robinson, D. Uptake and assimilation of nitrogen from solutions containing multiple N sources. *Plant Cell Environ.* **2005**, *28*, 813–821. [\[CrossRef\]](#)
38. Ma, Q.; Wang, J.; Sun, Y.; Yang, X.; Ma, J.; Li, T.; Wu, L. Elevated CO₂ levels enhance the uptake and metabolism of organic nitrogen. *Physiol. Plant.* **2017**, *162*, 467–478. [\[CrossRef\]](#)
39. Takatani, N.; Ito, T.; Kiba, T.; Mori, M.; Miyamoto, T.; Maeda, S.I.; Omata, T. Effects of high CO₂ on growth and metabolism of *Arabidopsis* seedlings during growth with a constantly limited supply of nitrogen. *Plant Cell Physiol.* **2013**, *55*, 281–292. [\[CrossRef\]](#)
40. Teng, N.; Wang, J.; Chen, T.; Wu, X.; Wang, Y.; Lin, J. Elevated CO₂ induces physiological, biochemical and structural changes in leaves of *Arabidopsis thaliana*. *New Phytol.* **2006**, *172*, 92–103. [\[CrossRef\]](#)
41. Weigel, H.J.; Manderscheid, R. Crop growth responses to free air CO₂ enrichment and nitrogen fertilization: Rotating barley, ryegrass, sugar beet and wheat. *Eur. J. Agron.* **2012**, *43*, 97–107. [\[CrossRef\]](#)
42. Li, S.; Li, Y.; He, X.; Li, Q.; Liu, B.; Ai, X.; Zhang, D. Response of water balance and nitrogen assimilation in cucumber seedlings to CO₂ enrichment and salt stress. *Plant Physiol. Biochem.* **2019**, *139*, 256–263. [\[CrossRef\]](#)
43. Vega-Mas, I.; Pérez-Delgado, C.M.; Marino, D.; Fuertes-Mendizábal, T.; González-Murua, C.; Marquez, A.J.; Betti, M.; Estavillo, J.M.; González-Moro, M.B. Elevated CO₂ Induces Root Defensive Mechanisms in Tomato Plants When Dealing with Ammonium Toxicity. *Plant Cell Physiol.* **2017**, *58*, 2112–2125. [\[CrossRef\]](#)
44. Pan, R.C.; Wang, X.Q.; Li, N.H. *Plant Physiology*; Higher Education Press: Beijing, China, 2012; pp. 23–36.
45. Torralbo, F.; Vicente, R.; Morcuende, R.; González-Murua, C.; Aranjuelo, I. C and N metabolism in barley leaves and peduncles modulates responsiveness to changing CO₂. *J. Exp. Bot.* **2018**, *70*, 599–611. [\[CrossRef\]](#) [\[PubMed\]](#)
46. Pérez-López, U.; Robredo, A.; Miranda-Apodaca, J.; Lacuesta, M.; Muñoz-Rueda, A.; Petite, A.M. Carbon dioxide enrichment moderates salinity-induced effects on nitrogen acquisition and assimilation and their impact on growth in barley plants. *Environ. Exp. Bot.* **2013**, *87*, 148–158. [\[CrossRef\]](#)
47. Zaghdoud, C.; Carvajal, M.; Ferchichi, A.; Ballesta, M.M. Water balance and N-metabolism in broccoli (*Brassica oleracea* L. var. Italica) plants depending on nitrogen source under salt stress and elevated CO₂. *Sci. Total. Environ.* **2016**, *571*, 763–771. [\[CrossRef\]](#) [\[PubMed\]](#)
48. Anabel, R.; Usue, P.; Jon, M.; Maite, L.; Amaia, M.; Alberto, M. Elevated CO₂ reduces the drought effect on nitrogen metabolism in barley plants during drought and subsequent recovery. *Environ. Exp. Bot.* **2011**, *13*, 399–408.
49. Vicente, R.; Pérez, P.; Martínez-Carrasco, R.; Usadel, B.; Kostadinova, S.; Morcuende, R. Quantitative RT-PCR Platform to Measure Transcript Levels of C and N Metabolism-Related Genes in Durum Wheat: Transcript Profiles in Elevated [CO₂] and High Temperature at Different Levels of N Supply. *Plant Cell Physiol.* **2015**, *56*, 1556–1573. [\[CrossRef\]](#) [\[PubMed\]](#)
50. Reyes, T.H.; Pompeiano, A.; Pompeiano, A.; Ciurli, A.; Lu, Y.; Guglielminetti, L.; Yamaguchi, J. Nitrate Reductase Modulation in Response to Changes in C/N Balance and Nitrogen Source in *Arabidopsis*. *Plant Cell Physiol.* **2018**, *59*, 1248–1254. [\[CrossRef\]](#)

51. Koch, M.; Naumann, M.; Pawelzik, E.; Gransee, A.; Thiel, H. The Importance of Nutrient Management for Potato Production Part I: Plant Nutrition and Yield. *Potato Res.* **2019**, *63*, 97–119. [[CrossRef](#)]
52. Di Martino, C.; Fioretto, A.; Palmieri, D.; Torino, V.; Palumbo, G. Influence of Tomato Plant Mycorrhization on Nitrogen Metabolism, Growth and Fructification on P-Limited Soil. *J. Plant Growth Regul.* **2019**, *38*, 1183–1195. [[CrossRef](#)]
53. Batnini, M.; Lopez-Gomez, M.; Palma, F.; Haddoudi, I.; Kallala, N.; Zribi, K.; Mrabet, M.; Mhadhbi, H. Sinorhizobium spp inoculation alleviates the effect of Fusarium oxysporum on Medicago truncatula plants by increasing antioxidant capacity and sucrose accumulation. *Appl. Soil Ecol.* **2020**, *150*, 103458. [[CrossRef](#)]
54. Agtuca, B.J.; Stopka, S.; Tuleski, T.R.; Amaral, F.P.D.; Evans, S.; Liu, Y.; Xu, D.; Monteiro, R.A.; Koppelaar, D.W.; Tolic, L.P.; et al. In-Situ Metabolomic Analysis of Setaria viridis Roots Colonized by Beneficial Endophytic Bacteria. *Mol. Plant-Microbe Interact.* **2020**, *33*, 272–283. [[CrossRef](#)] [[PubMed](#)]
55. Moran-Duran, S.A.; Flynn, R.P.; Heerema, R.; VanLeeuwen, D. Leaf Net Photosynthesis, Leaf Greenness, and Shoot Lignin Content of Nonbearing Pecan Trees at Two Nitrogen and Nickel Application Rates. *HortScience* **2020**, *55*, 231–236. [[CrossRef](#)]
56. Taiz, L.; Zeiger, E. *Plant Physiology*; Sinauer Associates Press: North Carolina, NY, USA, 2006; pp. 57–78.



© 2020 by the authors. Licensee MDPI, Basel, Switzerland. This article is an open access article distributed under the terms and conditions of the Creative Commons Attribution (CC BY) license (<http://creativecommons.org/licenses/by/4.0/>).